AMERICAN SOCIETY FOR MICROBIOLOGY | Molecular and Cellular Biology®

RESEARCH ARTICLE

Assembly of SNAPc, Bdp1, and TBP on the U6 snRNA Gene Promoter in *Drosophila melanogaster*

Mun Kyoung Kim,[a] An Tranvo,[a] Ann Marie Hurlburt,[b] Neha Verma,[b] Phuc Phan,[a] Jie Luo,[c] Jeff Ranish,[c] William E. Stumph[a]

[a]Department of Chemistry and Biochemistry and Molecular Biology Institute, San Diego State University, San Diego, California, USA
[b]Department of Biology and Molecular Biology Institute, San Diego State University, San Diego, California, USA
[c]Institute for Systems Biology, Seattle, Washington, USA

ABSTRACT U6 snRNA is transcribed by RNA polymerase III (Pol III) and has an external upstream promoter that consists of a TATA sequence recognized by the TBP subunit of the Pol III basal transcription factor IIIB and a proximal sequence element (PSE) recognized by the small nuclear RNA activating protein complex (SNAPc). Previously, we found that *Drosophila melanogaster* SNAPc (DmSNAPc) bound to the U6 PSE can recruit the Pol III general transcription factor Bdp1 to form a stable complex with the DNA. Here, we show that DmSNAPc-Bdp1 can recruit TBP to the U6 promoter, and we identify a region of Bdp1 that is sufficient for TBP recruitment. Moreover, we find that this same region of Bdp1 cross-links to nucleotides within the U6 PSE at positions that also cross-link to DmSNAPc. Finally, cross-linking mass spectrometry reveals likely interactions of specific DmSNAPc subunits with Bdp1 and TBP. These data, together with previous findings, have allowed us to build a more comprehensive model of the DmSNAPc-Bdp1-TBP complex on the U6 promoter that includes nearly all of DmSNAPc, a portion of Bdp1, and the conserved region of TBP.

KEYWORDS SNAPc-Bdp1 interaction, TBP recruitment, transcription factor assembly, U6 preinitiation complex, U6 small nuclear RNA transcription

RNA polymerase III (Pol III) transcribes genes for tRNAs, 5S rRNA, and various small nuclear RNAs (snRNAs). Genes for the tRNAs and 5S rRNA have gene-internal promoters that usually are TATA-less (1–3). However, other genes, including U6 snRNA, 7SK RNA, $tRNA^{sel}$, H1, and MRP RNAs, have gene-external promoters that consist of two distinct elements, a TATA sequence and a proximal sequence element (PSE) centered about 30 and 55 bp, respectively, upstream of the transcription start site (3–11). The TATA sequence is recognized by the Pol III general transcription factor TFIIIB (1–3), and the PSE is recognized by the small nuclear RNA activating protein complex (SNAPc) (10–16).

TFIIIB contains three subunits, most often TBP, Brf1, and Bdp1 (1–3). These three subunits form an architectural scaffold for Pol III recruitment and together coordinate conformational changes that lead to the formation of an open complex (17). Interestingly, depending upon the type of gene and/or the organism, TFIIIB can exhibit subunit heterogeneity. For example, in the fruit fly *Drosophila melanogaster*, the TFIIIB that assembles on Pol III genes that have internal promoters contains the TBP-related factor 1 (TRF1) in place of TBP (18). However, U6 and U6-type genes with external promoters utilize a TFIIIB that contains the canonical TBP rather than TRF1 (19). In another example, human Pol III-transcribed genes with internal promoters utilize a TFIIIB that contains canonical Brf1, whereas Pol III-transcribed snRNA genes require an alternative Brf known as Brf2 (20).

SNAPc is a multisubunit factor that binds to the PSE (termed the PSEA in fruit flies, the subject of this paper) to activate the transcription of snRNA genes (21–23). *D.*

Citation Kim MK, Tranvo A, Hurlburt AM, Verma N, Phan P, Luo J, Ranish J, Stumph WE. 2020. Assembly of SNAPc, Bdp1, and TBP on the U6 snRNA gene promoter in *Drosophila melanogaster*. Mol Cell Biol 40:e00641-19. https://doi.org/10.1128/MCB.00641-19.

Address correspondence to William E. Stumph, wstumph@sdsu.edu

Received 19 December 2019
Returned for modification 16 January 2020
Accepted 27 March 2020
Accepted manuscript posted online 6 April 2020
Published 28 May 2020

melanogaster SNAPc (DmSNAPc) consists of three subunits, DmSNAP190, DmSNAP50, and DmSNAP43, that are homologs of the three essential subunits of human SNAPc (14, 24–26). Although all three DmSNAPc subunits are required for DNA-binding activity, little is understood of the specific roles that the individual fly or human SNAPc subunits play in the recruitment of TFIIIB and the transcriptional activation of snRNA genes.

Previously, by using site-specific protein-DNA photo-cross-linking assays, we identified nucleotide positions where each of the individual DmSNAPc subunits cross-linked as part of the complex to U6 snRNA gene promoter DNA (14, 33). Likewise, we reported interactions of the TFIIIB subunits (in the absence of DmSNAPc) with specific nucleotides in the U6 snRNA gene promoter (28). Those studies revealed both the linear positions (translational location along the DNA helix) and rotational positions (face of the DNA double helix) occupied by each of the DmSNAPc and TFIIIB subunits on the DNA. Furthermore, by cleaving the DmSNAPc proteins at specific sites after photo-cross-linking, we were able to identify domains or regions of DmSNAP190, DmSNAP50, and DmSNAP43 that cross-linked to specific nucleotides within or adjacent to the PSEA (29–31).

Finally, in more recent work, we found that DmSNAPc can recruit Bdp1 to the U6 snRNA gene promoter in the absence of TBP and Brf1 (32). Furthermore, we identified an 87-amino-acid region of Bdp1 that was required for Bdp1 to be recruited to the U6 snRNA gene promoter by DmSNAPc (32). Over the years, this has allowed us to build a more and more encompassing picture of the architecture of the protein-DNA complex assembled on the U6 promoter (29, 31–33).

Given the findings from that previous work, we have now examined the recruitment of TBP to the U6 snRNA gene promoter by the DmSNAPc-Bdp1 complex. Furthermore, we applied site-specific protein-DNA photo-cross-linking assays to map the DmSNAPc, Bdp1, and TBP interactions with specific nucleotides of the U6 promoter. Finally, we examined the architecture of both the DmSNAPc-Bdp1-U6 promoter complex and the DmSNAPc-Bdp1-TBP-U6 promoter complex by applying cross-linking mass spectrometry (CXMS). The results of these studies allowed us to develop a more detailed model of the Pol III transcriptional machinery assembled on the U6 snRNA gene promoter that includes nearly all of DmSNAPc and parts of the TFIIIB components Bdp1 and TBP.

The canonical pathway for the assembly of the Pol III preinitiation complex (PIC) on tRNA genes involves the binding of TFIIIC to the gene-internal promoter followed by recruitment of TFIIIB (either preassembled or assembled in a stepwise process that involves the initial recruitment of Brf1 and TBP, followed by Bdp1 in a subsequent step) and finally RNA polymerase (2, 3, 34). (PIC assembly on 5S genes is believed to be similar but requires the prior binding of TFIIIA to aid in the recruitment of TFIIIC.) In contrast, our results raise the interesting possibility that PIC assembly on Pol III genes with external promoters in *D. melanogaster* proceeds by an alternate pathway that involves the following initial steps: first, DmSNAPc binds to the PSEA; second, DmSNAPc recruits Bdp1; and third, the promoter-bound DmSNAPc-Bdp1 complex and the TATA box recruit TBP. Brf1 and RNA polymerase may, in turn, assemble on the promoter at a subsequent step of PIC formation.

RESULTS

The DmSNAPc-Bdp1 complex can recruit TBP to the U6 promoter. Recently published data from our laboratory revealed that DmSNAPc can recruit Bdp1 to form a stable DmSNAPc-Bdp1 complex on the U6 gene promoter in the absence of TBP and Brf1 (32). To follow up that observation, we have now examined whether the DmSNAPc-Bdp1 complex plays a direct role in the recruitment of TBP to U6 promoter DNA. To that end, electrophoretic mobility shift assays (EMSAs) were performed (Fig. 1A) in which increasing amounts of TBP were incubated with the U6 promoter probe DNA in the absence (lanes 9 to 11) or presence (lanes 3 to 5) of DmSNAPc or both DmSNAPc and Bdp1 (lanes 6 to 8). Two reactions (lanes 12 and 13) contained still larger amounts of TBP and demonstrated that these larger amounts of TBP could bind to the U6 probe in the absence of other proteins.

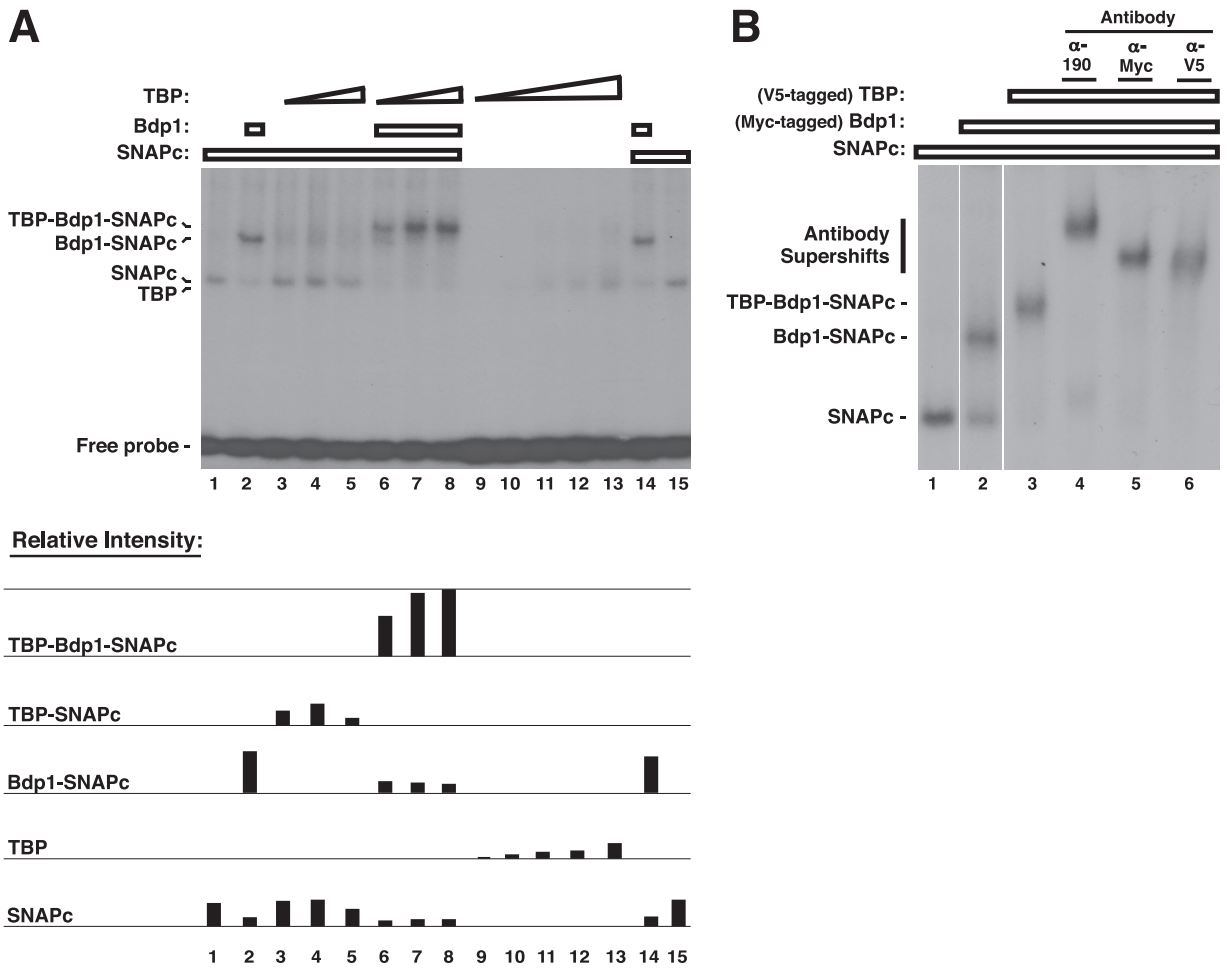

FIG 1 DmSNAPc-Bdp1 complex efficiently recruits TBP to the U6 promoter. (A) EMSA reactions with a wild-type U6 promoter DNA probe and increasing amounts of TBP (0.25, 0.5, and 0.75 μl) added in the presence of 3 μl DmSNAPc (lanes 3 to 5), in the presence of both 3 μl DmSNAPc and 2.5 μl Bdp1 (lanes 6 to 8), or TBP with no additional proteins (lanes 9 to 11). Lanes 12 and 13 show reactions with larger amounts of TBP (1 μl and 1.5 μl, respectively) to reveal the binding of TBP alone to the probe. Lanes 1 and 15 show reactions with DmSNAPc alone, and lanes 2 and 14 show reactions that contained DmSNAPc and Bdp1 together but no TBP. Results from quantitation of the relative band intensities by densitometry are shown in the lower part of the figure. It is possible that the lowest shifted band in lanes 3 to 8 includes some contribution from TBP, but even so, the conclusions from the experiment are unaffected. (B) EMSAs with specific antibody supershifts are shown. Each reaction mixture contained 3 μl DmSNAPc; lanes 2 to 6 each contained 2.5 μl of Bdp1; and lanes 3 to 6 each contained 0.5 μl of TBP. The TBP-Bdp1-DmSNAPc complex (lane 3) was supershifted by 1.5 μl of antibody against either DmSNAPc (α-190, lane 4), Bdp1 (α-Myc, lane 5), or TBP (α-V5, lane 6). Free probe was run off the gel to improve the resolution among the shifted bands. Lanes 1 and 2, although nonadjacent, are both from the same gel as lanes 3 to 6.

Reactions that contained the smaller amounts of TBP alone exhibited only very weak gel shifts (Fig. 1A, lanes 9 to 11). When the same amounts of TBP used in these reactions were added to a constant amount of DmSNAPc (Fig. 1A, lanes 3 to 5), clear DmSNAPc bands were observed together with a very light smear of slower-migrating bands that likely correspond to DNA fragments cooccupied by DmSNAPc and TBP (32). Importantly, when Bdp1 was present together with DmSNAPc and TBP, even the smallest amount of TBP was sufficient to form a higher-order and stronger complex of slower mobility (Fig. 1A, lanes 6 to 8). Moreover, essentially all the DmSNAPc bandshift seen in lanes 3 to 5 was supershifted into the higher-order complex in lanes 6 to 8. The addition of Bdp1 to TBP without DmSNAPc produced no bandshift beyond that seen with TBP alone (data not shown). The quantitation of these results (Fig. 1A, lower section) indicates that TBP is more efficiently recruited to the U6 promoter DNA by DmSNAPc and Bdp1 than DmSNAPc alone (lanes 6 to 8 versus lanes 3 to 5). These results indicate that Bdp1 can cooperate with DmSNAPc to recruit TBP to the U6 promoter.

The presence of all three proteins in the higher-order complex was confirmed by antibody supershifts (Fig. 1B). The TBP-Bdp1-DmSNAPc complex migrated more slowly

than the Bdp1-DmSNAPc complex (Fig. 1B, lane 3 versus lane 2), and this complex was further supershifted by antibodies against either DmSNAP190, the Myc epitope on Bdp1, or the V5 epitope on TBP (Fig. 1B, lanes 4, 5, and 6, respectively).

An 87-amino-acid region of Bdp1 between residues 424 and 510 is sufficient for TBP recruitment to the DmSNAPc-U6 promoter complex. We next investigated whether a specific region of Bdp1 is involved in recruiting TBP to the DmSNAPc-U6 promoter complex. Six Bdp1 constructs that had truncations exclusively at either the N or C terminus first were examined for their ability to recruit TBP. Previously, we found that DmSNAPc was able to recruit each of these six constructs to U6 promoter DNA, whereas Bdp1 constructs with further truncations from either the N or C terminus were not recruited (32). The upper panels of Fig. 2 (lanes 1 to 20) show that each of these Bdp1 truncation mutants was able to recruit TBP to form a higher-order complex with DmSNAPc on the U6 promoter (bands indicated with small circles). Quantitation of the results (table at the bottom of Fig. 2) suggests that the deletion of Bdp1 sequences located N-terminal of residue 335 or C-terminal of 510 actually increases the ability of the remaining Bdp1 sequences [constructs Bdp1(335-695) and Bdp(1-510)] to recruit TBP. This prompted us to further investigate the role of Bdp1 residues 335 to 510 in TBP recruitment.

For the next experiments, we used three Bdp1 constructs that contained either residues 335 to 510, only residues 335 to 424 (the SANT domain), or only residues 424 to 510. The two constructs that contained Bdp1 residues 424 to 510 formed a stable complex with DmSNAPc that recruited TBP to the U6 promoter as well as or better than the wild type (Fig. 2, lanes 24 to 27, bands indicated by circles; also see quantitation at the bottom). In contrast, the construct that contained only the SANT domain had little, if any, ability to recruit TBP in concert with DmSNAPc (Fig. 2, lanes 28 and 29). These results, together with those previously published (32), indicate that residues 424 to 510 are sufficient both for Bdp1 to interact with DmSNAPc and to recruit TBP.

It is nonetheless entirely possible that the SANT domain partially contributes to the efficiency of TBP recruitment. For example, we noticed a reproducible reduction in the intensity of the TBP-Bdp1-DmSNAPc band in the case of constructs that lacked the SANT domain compared to similar constructs that contained the SANT domain [Fig. 2, construct Bdp1(424-695) in lane 12 versus Bdp1(335-695) in lane 10 and construct Bdp1(424-510) in lane 27 versus construct Bdp1(335-510) in lane 25; also see quantitation at the bottom]. This is not surprising, because crystal and cryoelectron microscopy (cryo-EM) structures indicate that the human and yeast Bdp1 SANT domains directly contact TBP (17, 35, 36).

The importance of Bdp1 residues 424 to 510 for recruitment of Bdp1 and TBP by DmSNAPc was further investigated by using a construct [Bdp1Δ(424-510)] that contained an internal deletion of only the 87 residues from 424 to 510 (last construct illustrated in the upper section of Fig. 2). The wild-type and deletion constructs were normalized by Western blotting against the FLAG epitope and used in side-by-side assays together with DmSNAPc and TBP (Fig. 2, lanes 33 to 39). DmSNAPc was unable to recruit Bdp1Δ(424-510), whereas it did recruit the wild-type Bdp1 (lanes 34 and 35). Similarly, in contrast to the wild-type Bdp1, Bdp1Δ(424-510) was unable to cooperate with DmSNAPc to recruit TBP (lanes 36 and 37), even though the deletion construct contained all of the Bdp1 sequence except amino acid residues 424 to 510. Thus, the remaining 608 residues of Bdp1 (residues 1 to 423 and 511 to 695 together) cannot compensate for the loss of the 87 amino acids from 424 to 510 with respect to Bdp1 and TBP recruitment to the DmSNAPc-U6 promoter complex.

TBP recruitment by the DmSNAPc-Bdp1 complex requires a TATA box. We next investigated whether TBP recruitment under such circumstances was also dependent upon the presence of the TATA box in the U6 promoter. For this, a DNA EMSA probe was used that was identical to the wild-type probe, except the TATA sequence (TTTATATA) was mutated to GGGACCTC. As expected, TBP by itself was able to bind to the wild-type probe but did not bind to the mutant TATA probe (Fig. 3A, lanes 1 and

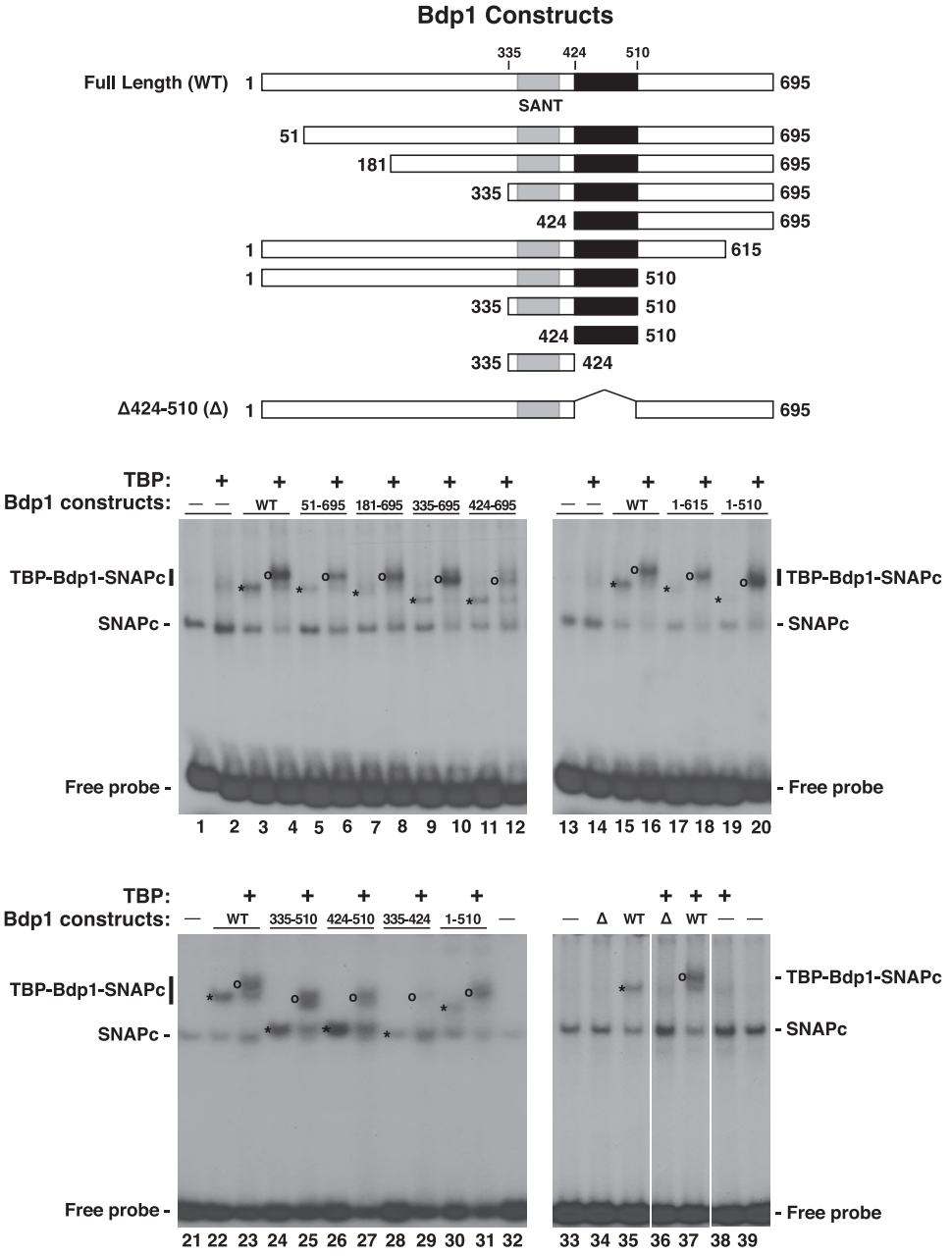

Bdp1 Construct:	WT	51-695	181-695	335-695	424-695	1-615	1-510	335-510	424-510	335-424
Rel. efficiency of TBP recruitment:	1.0	1.1	0.9	2.1	1.1	1.5	3.2	1.9	0.9	0.2

FIG 2 Eighty-seven-residue region of Bdp1 just C-terminal of the SANT domain is sufficient for TBP recruitment in the presence of DmSNAPc. EMSAs are shown that utilized various Bdp1 truncation constructs together with DmSNAPc and full-length TBP. At the top of the figure, truncated Bdp1 constructs utilized in EMSAs are illustrated as long rectangles. The location of the highly conserved SANT domain is indicated by a gray box within each construct, and the region identified as important for DmSNAPc recruitment of Bdp1 (amino acid residues 424 to 510) (32) is indicated by the black box within each construct. The particular Bdp1 construct utilized in each lane is indicated above the respective lanes and varied between 2 μl and 7 μl. Reactions run in all lanes contained DmSNAPc (3 μl). TBP (0.5 μl) was added to the reaction mixtures loaded in the lanes indicated by plus signs. The circles indicate the positions of the bands that correspond to the complexes formed by DmSNAPc together with TBP and the various truncation constructs of Bdp1. The asterisks, on the other hand, indicate the bands that correspond to DmSNAPc-Bdp1 complexes on the DNA that do not include TBP. Lanes 33 to 39 are all from the same exposure of the same gel. Quantitation of the results of lanes 1 to 32 is shown at the bottom of the figure and represents the ratio (relative to the wild type, normalized to 1.0) of the TBP-Bdp1-DmSNAPc-U6 promoter complex to the Bdp1-DmSNAPc-U6 promoter complex in the same lane.

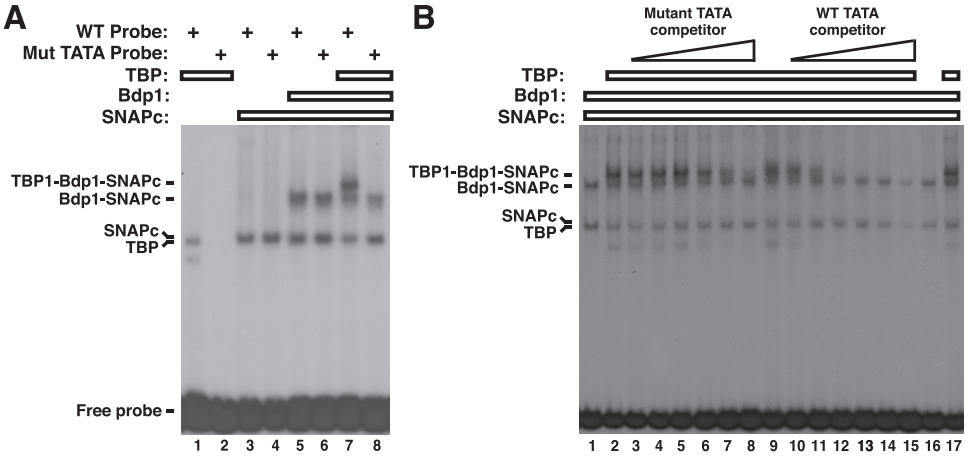

FIG 3 TBP recruitment to the U6 promoter by DmSNAPc-Bdp1 requires a TATA box. (A) Shown is an EMSA that utilized either the wild-type U6 promoter probe (odd-numbered lanes) or a probe that was identical to the wild-type sequence with the exception of a mutated TATA box (even-numbered lanes). Each probe was incubated with either 3 μl of DmSNAPc alone (lanes 3 and 4), 3 μl of DmSNAPc together with 2 μl of Bdp1 (lanes 5 and 6), or 3 μl of DmSNAPc together with 2 μl of Bdp1 and 0.4 μl of TBP (lanes 7 and 8). Each probe was also incubated with 1 μl of TBP alone (lanes 1 and 2). The identities of the shifted bands and free probe are indicated to the left of the panel. (B) Unlabeled wild-type or mutant TATA-containing oligonucleotides were used as competitors in EMSAs to further examine the requirement of a TATA box for TBP recruitment to the U6 promoter. Each reaction mixture contained 1 μl DmSNAPc and 2 μl Bdp1. All other reaction mixtures also contained 1.2 μl of TBP, with the exception of the reaction mixtures shown in lanes 1 and 16. Unlabeled competitor oligonucleotides were added in increasing amounts (1.5, 5.0, 15, 50, 150, and 500 ng) to lanes 3 through 8 (mutant TATA competitor) and to lanes 10 through 15 (wild-type TATA competitor).

2). On the other hand, DmSNAPc bound equally well to both the wild-type and mutant TATA probes (Fig. 3A, lanes 3 and 4). Interestingly, the mutation of the TATA sequence had no effect on the recruitment of Bdp1 by DmSNAPc (Fig. 3A, lanes 5 and 6). In stark contrast, the DmSNAPc-Bdp1 complex effectively recruited TBP to the wild-type promoter but was unable to recruit TBP to the mutant TATA promoter (Fig. 3A, compare lanes 7 and 8). These results indicate that the recruitment of TBP, but not Bdp1, to the U6 promoter by DmSNAPc is dependent upon the presence of a TATA sequence. The results further strongly suggest that TBP directly interacts with the TATA sequence when it is recruited to the U6 promoter by DmSNAPc and Bdp1.

As an alternative method to examine the importance of the TATA box for TBP recruitment, EMSAs were performed with increasing amounts of unlabeled oligonucleotides that contained either the wild-type or the mutated TATA sequence (Fig. 3B). The competitor oligonucleotides lacked the PSEA sequence so as not to compete away binding of DmSNAPc (and Bdp1) to the labeled U6 promoter probe. The results indicate that the TBP-Bdp1-DmSNAPc band was competed away more effectively by the TATA-containing oligonucleotide than the oligonucleotide that contained a mutant TATA sequence (compare lanes 3 to 8 with lanes 10 to 15). Quantitation of the data (not shown) revealed that the oligonucleotide with the TATA sequence was a greater than 50-fold better competitor than the oligonucleotide with the mutated sequence, providing further evidence that the TATA sequence is essential for efficient TBP recruitment.

Identification of nucleotide positions where Bdp1 cross-links to the U6 snRNA gene promoter as part of a DmSNAPc-Bdp1-TBP-DNA complex. In previous work, we used site-specific protein-DNA photo-cross-linking assays to map the nucleotide positions of the U6 promoter that are in close proximity to the three different subunits of DmSNAPc when DmSNAPc alone is bound to the DNA (33). In a more recent study, we similarly mapped the nucleotide positions where each of the three subunits of TFIIIB map to the U6 promoter DNA when TFIIIB alone is bound to the DNA (28). To extend these data, we have now investigated the binding pattern of the DmSNAPc-Bdp1-TBP ternary protein complex on the U6 promoter DNA.

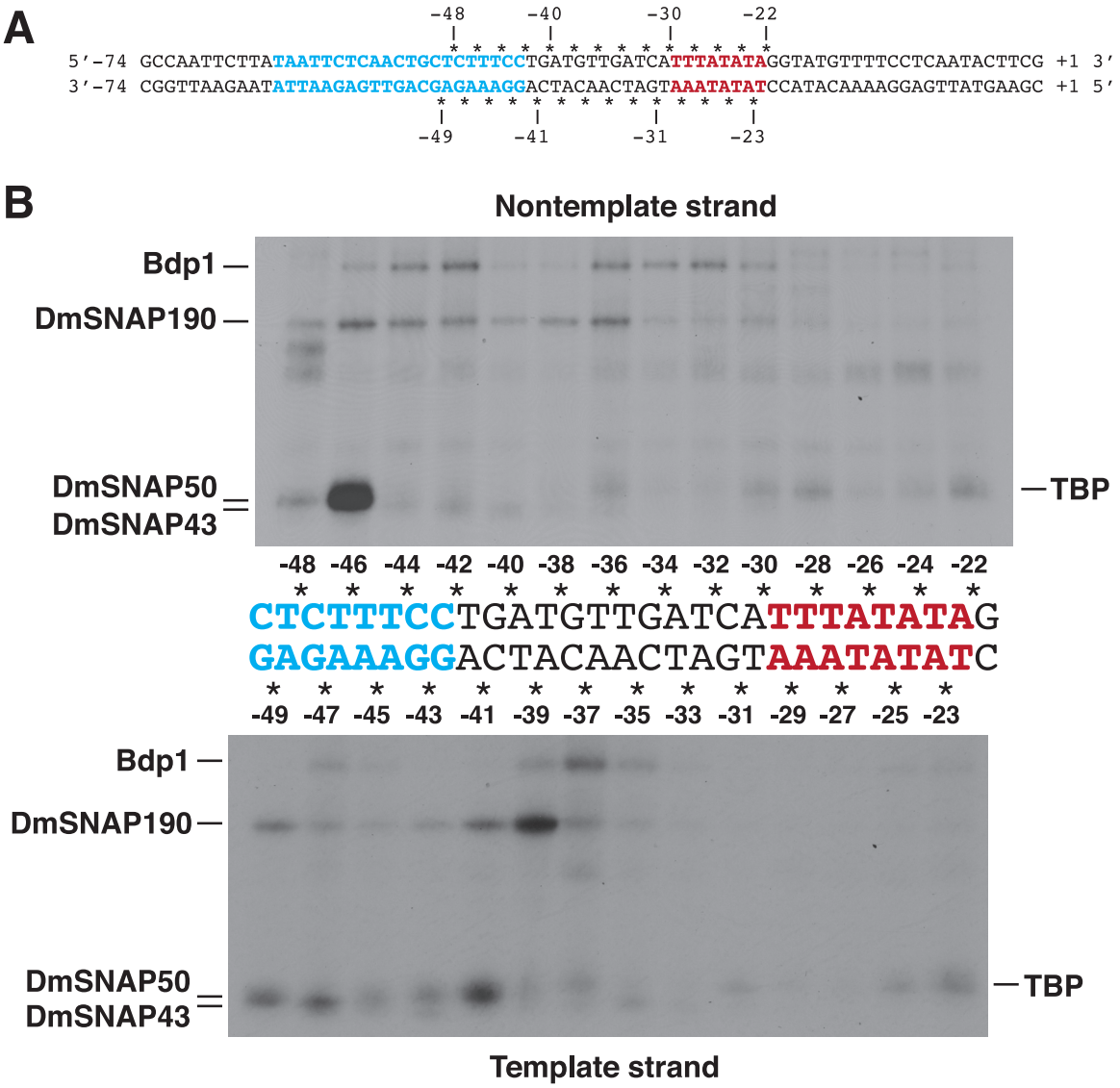

FIG 4 Site-specific protein-DNA photo-cross-linking of Bdp1 in a complex with DmSNAPc and TBP to the U6 snRNA gene promoter. (A) DNA probe used for protein-DNA photo-cross-linking assays. The cross-linker was placed individually at 28 different phosphate positions (14 on each strand), as indicated by the asterisks. The negative numbers indicate the nucleotide distance from the transcription start site. The PSEA is indicated with blue color, and the TATA box is indicated with red color. (B) Autoradiography of cross-linked Bdp1, DmSNAPc, and TBP to 28 nucleotide positions within the U6 snRNA gene promoter. The identities of the protein bands are indicated to the left of each panel (except for TBP, which cross-linked to nucleotides within and closely flanking the TATA box). The apparent cross-linking of DmSNAP190 to positions −42 and −40 was not seen when the reactions were done with DmSNAPc that contained FLAG-tagged DmSNAP43 rather than DmSNAP190 (data not shown). This indicates that there is an excess of FLAG-tagged DmSNAP190 in the experiments shown here due to the use of anti-FLAG resin for the purification of DmSNAPc.

To perform the site-specific protein-DNA photo-cross-linking assays, we prepared 28 different double-stranded DNA probes that contained the sequence of the promoter of the *D. melanogaster* U6:96Ab gene (Fig. 4A). Each probe contained a photo-cross-linking agent at a unique position in the phosphate backbone together with an adjacent radiolabel. The phosphate positions individually assayed by this procedure are indicated by the asterisks in Fig. 4A. Probes were coincubated with DmSNAPc, Bdp1, and TBP, irradiated with UV light, and subjected to nuclease digestion as previously described (33). Cross-linked proteins were identified by SDS-PAGE followed by autoradiography.

Figure 4B (upper) shows that Bdp1, when assembled with DmSNAPc and TBP, cross-linked to the nontemplate (upper) strand at positions −46 to −42 and −36 to

−30 with various intensities. On the template strand (Fig. 4B, lower), Bdp1 cross-linked to phosphate positions −47, −45, and −39 to −35, again with various intensities. The upper and lower strand patterns are highly consistent with each other under the assumption that Bdp1 interacts primarily with a single face of the DNA over the region examined in these experiments. The cross-linking of Bdp1 that occurred on both DNA strands at the positions near the TATA box was not surprising based on results we previously obtained with TFIIIB alone (28) and results observed by others from yeast TFIIIB cryo-EM structures (17).

Interestingly, the data also revealed that nucleotides farther upstream (phosphates −46, −44, −42, −47, and −45) also cross-linked to Bdp1. These phosphate positions are located within the 3′ half of the PSEA itself at nucleotides that also cross-link to one or more of the DmSNAPc subunits. From these protein-DNA photo-cross-linking results, it can be surmised that Bdp1 is near nucleotides in the 3′ portion of the U6 PSEA. This strongly suggests that a region of Bdp1 must lie in very close physical proximity to one or more subunits of DmSNAPc. This is consistent with the existence of direct protein-protein contacts that permit DmSNAPc to recruit Bdp1 to the U6 promoter (32).

With respect to the cross-linking of DmSNAPc to the DNA, the patterns of cross-linking of the DmSNAPc subunits in Fig. 4B is very similar to the cross-linking patterns of those previously reported by Wang and Stumph (33). The only noticeable difference is that DmSNAP190 cross-linked more strongly to position −36 in the presence of Bdp1 than DmSNAPc alone (14). This suggests that DmSNAP190 is more "locked down" on the DNA in the presence of Bdp1 than with DmSNAPc alone.

Residues 424 to 510 of Bdp1 cross-link to the U6 snRNA gene promoter upstream of the TATA box and within the PSEA. To identify the region(s) of Bdp1 that cross-linked to the U6 snRNA gene promoter upstream of the TATA box, we utilized several truncated Bdp1 proteins together with DmSNAPc and TBP in photo-cross-linking experiments. Because amino acid residues 424 to 510 of Bdp1 were implicated in both Bdp1 and TBP recruitment by DmSNAPc (Fig. 2) (32), we performed photo-cross-linking experiments with N-terminal and C-terminal truncations of Bdp1 that included or lacked this region (Fig. 5A). For these protein-DNA photo-cross-linking assays, we examined five nucleotide positions from each strand (phosphates −44, −42, −36, −34, and −32 on the nontemplate strand and phosphates −47, −45, −39, −37, and −35 on the template strand), positions where full-length Bdp1 had been observed to cross-link (Fig. 4).

Figure 5B shows that full-length Bdp1 as well as two Bdp1 constructs that contained amino acid residues 424 to 510 [Bdp1(424-695) and Bdp1(1-510)] each cross-linked strongly to all ten of the assayed positions. However, the two constructs that lacked these residues either did not detectably cross-link [Bdp1(511-695)] or yielded an extremely weak signal [Bdp1(1-423)].

Those results indicate that a region of Bdp1 between amino acid residues 424 and 510 is involved in the cross-linking interaction with the U6 snRNA gene promoter. To further examine this possibility, the construct Bdp1(424-510) was employed in cross-linking assays with the same ten phosphate positions used for Fig. 5B. Due to the small size of the construct, the cross-linked samples were run on higher-percentage gels (Fig. 5C). We observed that amino acid residues 424 to 510 of Bdp1, in a complex with DmSNAPc and TBP, cross-linked to each of these nucleotide positions (Fig. 5C, lanes 6 to 10 and lanes 16 to 20) where full-length Bdp1 cross-linked (lanes 1 to 5 and 11 to 15). Moreover, the pattern of cross-linking intensities with Bdp1(424-510) was very similar to that obtained with the full-length Bdp1. In conclusion, these findings indicate that an 87-amino-acid region of Bdp1 that is sufficient for Bdp1 recruitment by DmSNAPc is also in close proximity to the U6 promoter DNA upstream of the TATA box, apparently positioned there by an interaction with DmSNAPc.

When bound to U6 promoter DNA, Bdp1 residues 424 to 510 form an interface with DmSNAP43 and DmSNAP190. To further investigate regions of Bdp1 that may interact with DmSNAPc on the U6 promoter, we next used cross-linking mass spectrometry (CXMS). DmSNAPc and Bdp1 were coincubated together with U6 promoter

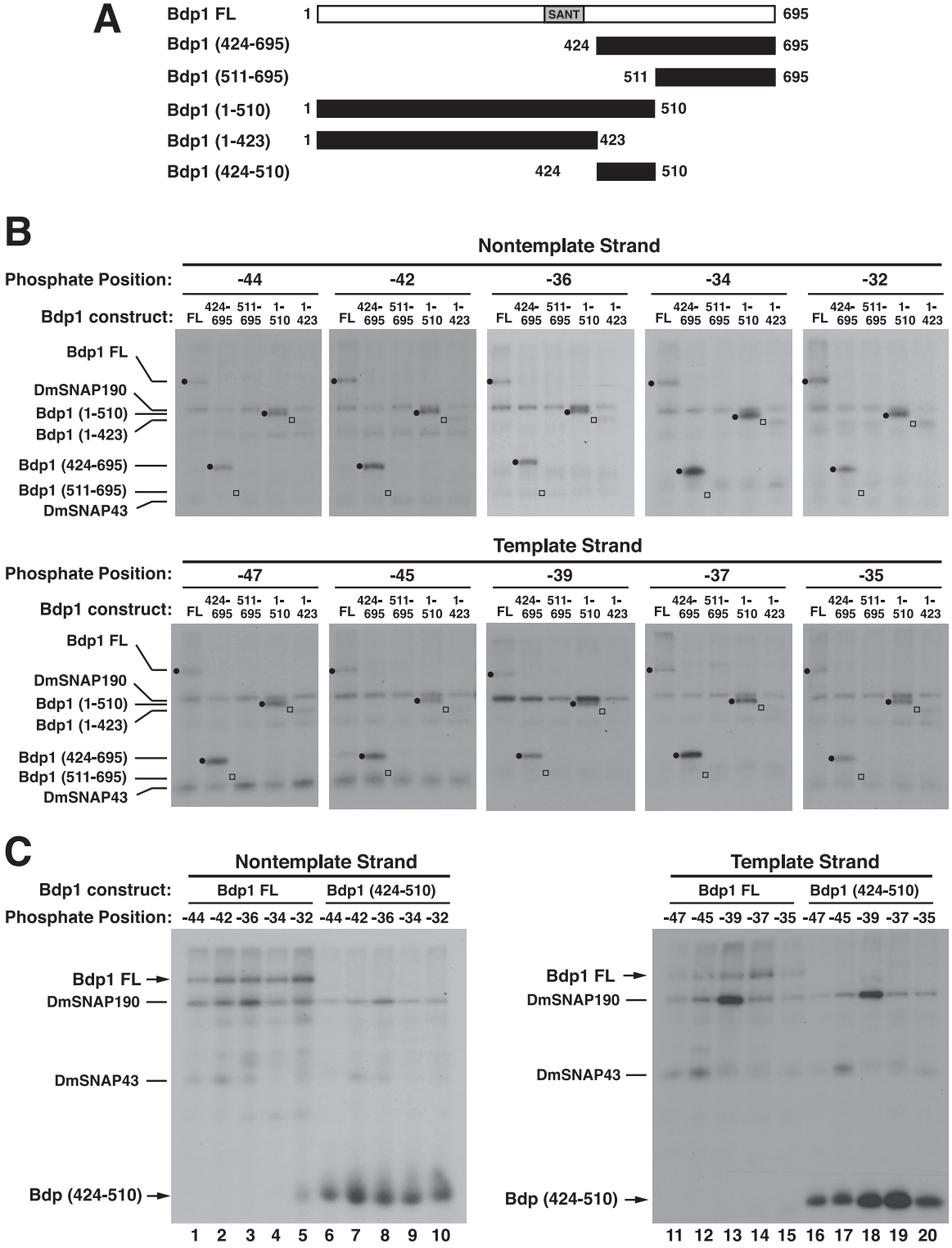

FIG 5 Site-specific protein-DNA photo-cross-linking of truncated Bdp1 constructs, DmSNAPc, and TBP at select nucleotide positions within the U6 snRNA gene promoter. (A) Truncation constructs used to identify a region of Bdp1 that cross-links to the U6 snRNA gene promoter in the presence of DmSNAPc and TBP. (B) Autoradiography of protein-DNA cross-linking reactions at ten nucleotide positions where full-length Bdp1 (Bdp1 FL) cross-linked (Fig. 4). In each panel, constructs that contained residues 424 to 510 [Bdp1 FL, Bdp1(424-695), and Bdp1(1-510)] cross-linked to each position examined (bands indicated by closed circles). On the other hand, constructs missing residues 424 to 510 did not cross-link or cross-linked extremely weakly. The positions where bands should appear for these constructs (determined by Western blotting) are indicated by squares. (C) Cross-linking of full-length Bdp1 (Bdp1 FL) and construct Bdp1(424-510) to the same 10 nucleotide positions as in panel B.

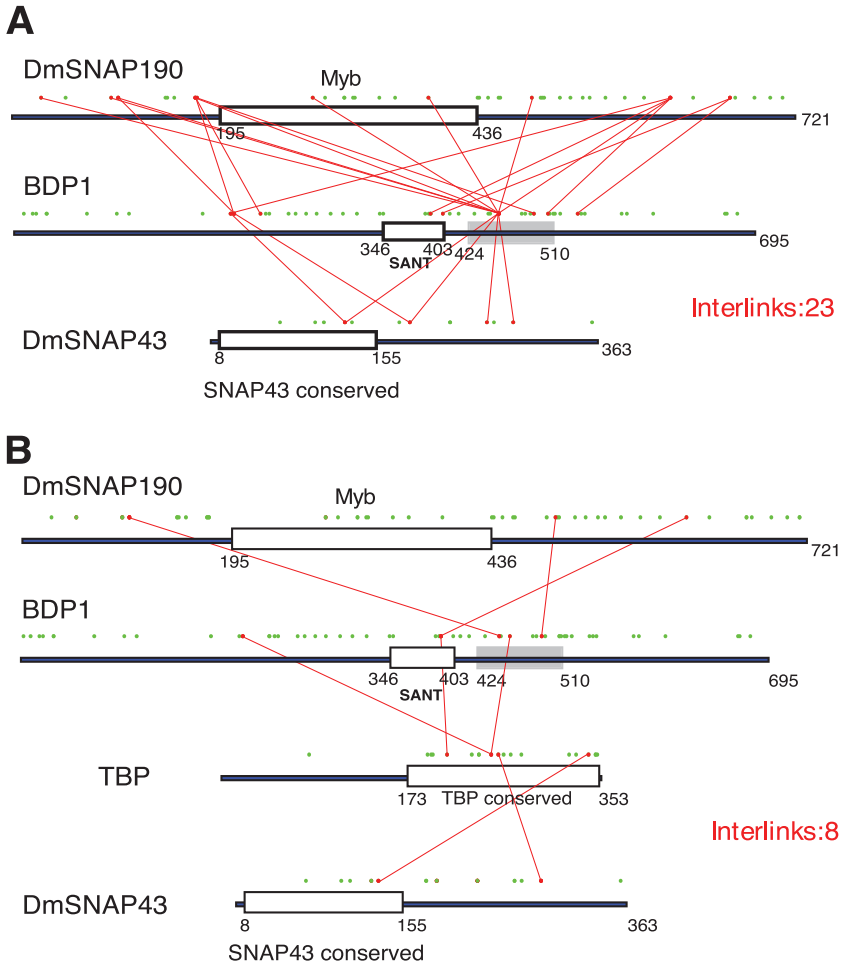

FIG 6 BS3 cross-linking map for the DmSNAPc-Bdp1-U6 promoter complex (A) and the DmSNAPc-Bdp1-TBP-U6 promoter complex (B). The green dots indicate the positions of lysine residues along the protein sequences. The red dots and lines between the dots indicate cross-linked lysine residues that were identified by mass spectrometry. The gray rectangle indicates the region of Bdp1 required for Bdp1 and TBP to be recruited to the U6 promoter by DmSNAPc (Fig. 2). Only cross-links involving Bdp1 and/or TBP are shown.

DNA. The complexes then were treated with the chemical cross-linker BS3, which can cross-link lysines that are in proximity to each other. No cross-links between Bdp1 and DmSNAP50 were identified (data not shown). However, we were able to identify 23 lysine-lysine cross-links between Bdp1 and either DmSNAP43 or DmSNAP190 (Fig. 6A).

Notably, 14 of the 23 Bdp1 cross-links are within the region of Bdp1 (residues 424 to 510) that is required for Bdp1 recruitment by DmSNAPc, and three additional cross-links involved lysines close to this region (424 to 510) (two from within the C-terminal part of the SANT domain). These results indicate that this region of Bdp1 is in close proximity to DmSNAP43 and DmSNAP190 and, together with results presented in Fig. 2 and 5, suggest that this region forms an interface with DmSNAP43 and DmSNAP190. The only other part of Bdp1 that cross-links to DmSNAPc in our experiments (6 cross-links) is a more N-terminal region that includes lysines between amino acids 203 and 231 (Fig. 6). These results indicate that a second region of Bdp1 N-terminal of the SANT domain is also in close proximity to DmSNAP43 and DmSNAP190; however, this region is not essential for a stable interaction with DmSNAPc on the U6 promoter (Fig. 2).

The DmSNAP190 cross-links to Bdp1 occur mostly within the regions N-terminal (eight cross-links) and C-terminal (seven cross-links) of the Myb domain, compared to only two cross-links within the Myb domain itself. Similarly, the majority of the

cross-links of DmSNAP43 to Bdp1 occur mainly within the nonconserved C-terminal portion of DmSNAP43. Together, these CXMS results suggest that the nonconserved N- and C-terminal regions of DmSNAP190 and the C-terminal region of DmSNAP43 are in close proximity to Bdp1 and may be involved in recruiting Bdp1. DmSNAP50, on the other hand, likely lies more distant from Bdp1 than DmSNAP190 and DmSNAP43. These results are in very good accord with the previously modeled locations of the DmSNAPc subunits on the U6 promoter that were based primarily upon protein-DNA photo-cross-linking (14, 29, 31, 33).

DmSNAP43 forms an interface with TBP in the DmSNAPc-Bdp1-TBP-U6 promoter complex. We next performed CXMS with TBP in the reaction together with DmSNAPc, Bdp1, and the U6 promoter. We identified 19 intersubunit links between DmSNAPc, Bdp1, and TBP. The majority of these were cross-links that involved the lysine-rich FLAG epitope tags (data not shown); however, eight cross-links involved residues within the natural coding regions of these proteins (Fig. 6B). Although fewer cross-links were identified in the sample containing TBP (Fig. 6B) than without TBP (Fig. 6A), the pattern of cross-linking between DmSNAP190 and Bdp1 is similar. The cross-link between TBP Lys:250 and Bdp1 Lys:455, within the region of residues 424 to 510, is consistent with the ability of this region of Bdp1 to recruit TBP to the U6 promoter (Fig. 2).

The cross-link of TBP to a lysine within Bdp1(203-231) suggests that this region of Bdp1 is close not only to DmSNAP190 and DmSNAP43 (Fig. 6A) but also to TBP. Finally, the cross-link between the Bdp1 SANT domain and TBP is consistent with the known interaction of the SANT domain with TBP (17).

Perhaps the most interesting aspect of the results shown in Fig. 6B is the two cross-links that indicate the proximity of DmSNAP43 to TBP. This is not unexpected based on the ability of DmSNAPc and TBP to form a complex on the U6 promoter (Fig. 1) (32). When taken together with the site-specific protein-DNA photo-cross-linking data, the results strongly suggest that DmSNAP43 is an elongated molecule that can both interact with the 3′ half of the PSEA and reach TBP on a downstream TATA box.

When TBP was present in the sample (Fig. 6B), no cross-links were observed between DmSNAP43 and Bdp1; this contrasts with the results obtained in the absence of TBP (Fig. 6A). Based on the available data, the explanation for this difference currently is not clear. While the change in the cross-linking pattern could be due to a conformational change in the complex or occlusion by TBP, it also could result from undersampling due to the complexity or the limited availability of the sample.

A model of DmSNAPc, Bdp1, and TBP on a *D. melanogaster* U6 snRNA gene promoter. The data presented here (from EMSAs, site-specific protein-DNA photo-cross-linking, and CXMS) allow us to develop a more complete and detailed model that builds upon a series of previous models of DmSNAPc bound to the U6 promoter (14, 29, 31, 33). Together, the data permit us to better integrate DmSNAPc with Bdp1 and TBP. Our updated understanding is shown in Fig. 7. This model contains nearly all of DmSNAPc, a portion of Bdp1, and the conserved region of TBP.

DmSNAP190 residues 1 to 441 (61% of the protein) could be modeled surprisingly well by the RaptorX structure prediction program (37) by using the crystal structure of the *Schizosaccharomyces pombe* Reb1 DNA-binding protein as a template (*P* value of 5.10e−05). DmSNAP190 is predicted to have structural similarity to Reb1 not only in its 4.5 Myb repeat region (residues 183 to 441, known as Myb repeats Rh, Ra, Rb, Rc, and Rd) but also in the DmSNAP190 N-terminal domain (residues 1 to 182). The latter domain of DmSNAP190 interacts extensively with the DNA (29–31), a feature shared with the homologous region of Reb1 (38). Therefore, we used the Reb1-templated structure of DmSNAP190 to model the first 441 residues of DmSNAP190 on the U6 PSEA (Fig. 7, protein residues shown in yellow).

Residues 1 to 182, previously modeled only as an unstructured oval, are positioned to interact with the 3′ half of the PSEA, in accordance with previous site-specific protein-DNA photo-cross-linking data (29–31). The 4.5 Myb repeats (residues 183 to 441) are placed on the DNA similarly to previous models that also relied upon

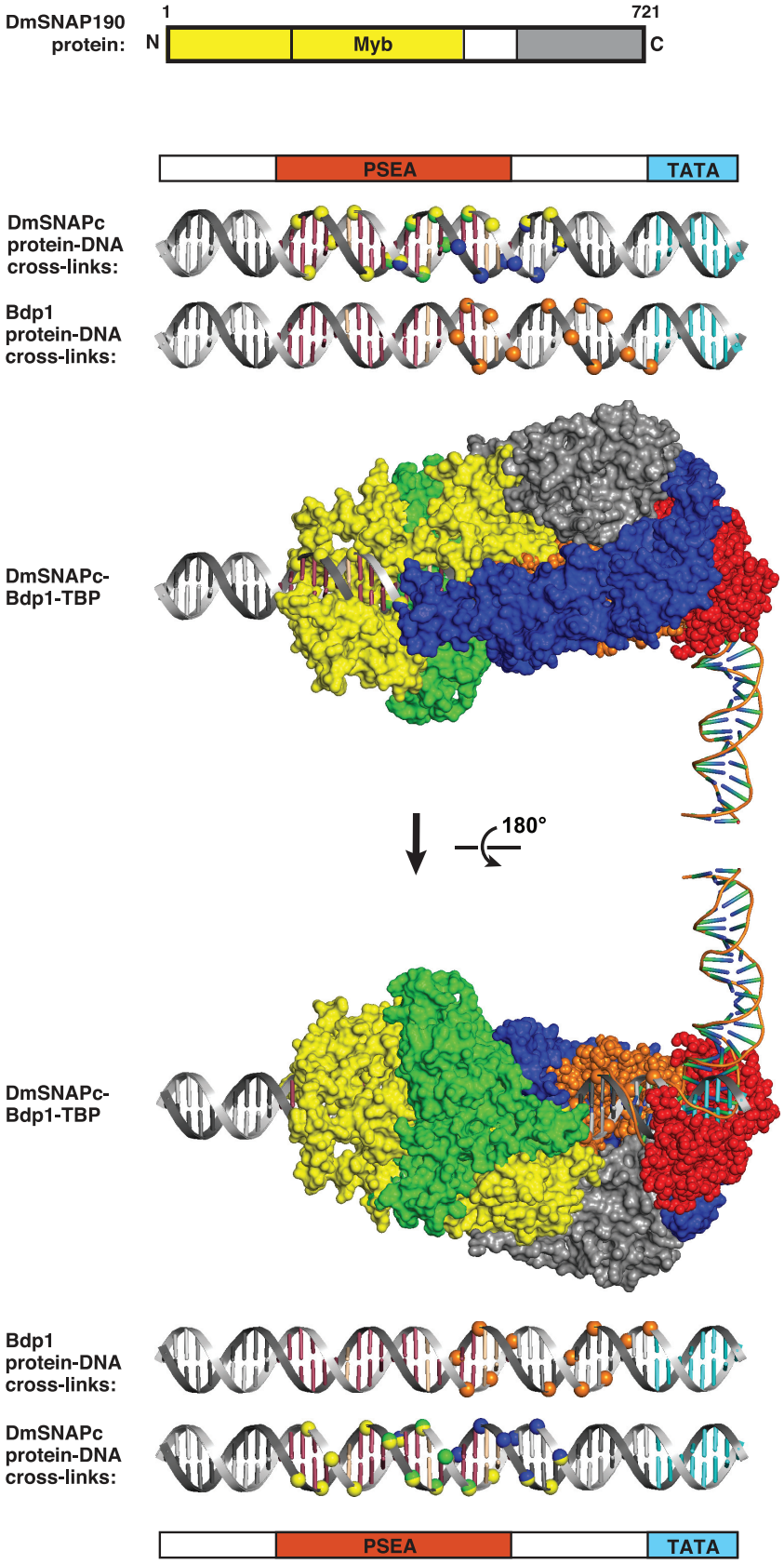

FIG 7 Model of a partial preinitiation complex assembled on the U6 snRNA gene promoter consistent with EMSAs, site-specific protein-DNA photo-cross-linking, and CXMS. DmSNAP190 is shown in yellow

(Continued on next page)

protein-DNA cross-linking experiments in which the location of each individual Myb repeat was mapped on the U6 promoter DNA (31).

The structure of DmSNAP50 is unknown, and there seems to be no template sufficient to model its structure. Previously we mapped specific segments of these proteins that photo-cross-link to specific nucleotides in the U6 promoter (29). We used RaptorX to generate *a priori* globular structures of segments of DmSNAP50 and placed these in position to cross-link to the proper nucleotides of the DNA, as previously mapped (29). We do not presume that the *a priori* model represents the actual secondary and tertiary structures of DmSNAP50, but we believe that the globular, correctly sized structures obtained from the modeling program can serve as proxies to localize segments of the protein on the DNA based upon our previous protein-DNA photo-cross-linking. The whole of DmSNAP50 was modeled and is shown in green in Fig. 7. The use of B-form DNA is reasonable, as previous work indicated that the DNA was only slightly bent by the binding of DmSNAPc (39).

Prior to modeling DmSNAP43, we inserted TBP and *D. melanogaster* Bdp1 into the structural model. We used a published yeast TFIIIB structure (17) and overlapped the nearly B-form yeast DNA that extends upstream of the TATA box with the B-form DNA that contains the PSEA. We aligned the sequences with the proper separation (i.e., 12 bp) between the PSEA and the TATA box (40). This alignment of the DNA allowed the visualization of yeast TBP (red in Fig. 7) at the correct distance and rotational position relative to DmSNAPc. Because this same yeast structure included the very highly conserved SANT domain of Bdp1, we used the yeast Bdp1 SANT domain as a three-dimensional template to insert the corresponding domain of *D. melanogaster* Bdp1 (orange in Fig. 7) into the structure, replacing the SANT domain of the yeast protein with the SANT domain of fly Bdp1. The globular SANT domain that lies just behind TBP can be seen in the lower image of Fig. 7. Although the structural models of the SANT domains from the two species overlapped very well, RaptorX revealed no structural homologies between yeast and fruit fly Bdp1 outside the SANT domains (data not shown).

Residues 424 to 510 of *D. melanogaster* Bdp1, which lie just C-terminal of the SANT domain, are required for the recruitment of Bdp1 and TBP by DmSNAPc (Fig. 2) (32). Moreover, they cross-linked to specific nucleotides located between and within the PSEA and the TATA box (Fig. 5). Finally, this region, together with residues immediately adjacent to it, cross-linked by CXMS to both the DmSNAP190 and DmSNAP43 subunits (but not to DmSNAP50) (Fig. 6A). Residues 424 to 510 of fly Bdp1 are predicted to be disordered and are absent from the RaptorX modeling of fly Bdp1. However, just

FIG 7 Legend (Continued)
and gray, DmSNAP50 in green, DmSNAP43 in blue, Bdp1 in orange, and TBP in red. At the top, the linear structure of DmSNAP190 is shown with DmSNAP190 residues 1 to 456 and 528 to 721 indicated in yellow and gray, respectively, to correspond to the same two regions of DmSNAP190 in the panels below. The entire DmSNAP50 and DmSNAP43 are shown in green and blue, respectively. The naked B-form DNA structures shown above the protein-DNA structure are based on the U6-96Ab gene sequence between positions −73 and −23. The nontemplate strand is shown in light gray and the template strand in dark gray. The U6 PSEA is indicated by raspberry-colored bases, except for the five bases (light orange) that differ from the U1-95.1 gene PSEA, and are important for Pol III versus Pol II specificity (32, 45–47). The TATA box bases are shown in cyan. The naked DNAs also show the phosphate positions to which DmSNAP43 (blue), DmSNAP50 (green), and DmSNAP190 (yellow) cross-linked in this and previous work. Many of the phosphate positions cross-linked to more than one DmSNAPc subunit; in that case, individual spheres contain more than one color. Shown separately in orange are the phosphate positions to which Bdp1 cross-linked. The portion of the DmSNAP190 structure shown in yellow is based upon that of the fission yeast Reb1 protein; flexible loops between Myb repeats were used to position the Myb repeats in concert with previous data (31). The gray portion of the DmSNAP190 structure represents the C-terminal 179 amino acid residues of DmSNAP190 modeled as a ligand-binding domain of a nuclear hormone receptor placed in accordance with CXMS DmSNAP190-Bdp1 SANT domain cross-links. DmSNAP50 and DmSNAP43 are structures generated as described in the text. and placed onto the DNA in locations consistent with previous and current site-specific protein-DNA photo-cross-linking. Constraints from CXMS data together with protein-DNA cross-linking indicate that DmSNAP43 has an extended structure stretching from the PSEA to the upper surface of TBP. The placement of TBP and Bdp1 into the combined structure is described in the main text.

beyond that region, there was an unstructured loop that we utilized as a proxy to model the region that contains residues 424 to 510. Although these are different amino acids, we sculpted this region to fit into our model near DmSNAP190 and DmSNAP43, where it could also cross-link to the DNA in a manner that would be consistent with our site-specific protein-DNA photo-cross-linking results (Fig. 4 and 5). Much of this elongated loop, which represents Bdp1(424-510), is obscured behind DmSNAP43 in the upper image of Fig. 7.

Returning to DmSNAP190, we found that the last 179 residues at the C terminus of DmSNAP190 (residues 543 to 721) could be modeled by RaptorX using the ligand binding domain of mammalian nuclear hormone receptors (e.g., human lipid X receptor beta, thyroid hormone receptor, and mouse estrogen-related receptor gamma) as templates (*P* value of 1.39e−02). More importantly, we identified two crucial CXMS lysine cross-links (Fig. 6A) that indicated that residues 618 and 673 of DmSNAP190 reside in proximity to Bdp1 residues 391 and 402, respectively. The latter two Bdp1 residues are within the SANT domain of fly Bdp1. Therefore, these CXMS data indicate that the C-terminal region of DmSNAP190 must lie reasonably close to the Bdp1 SANT domain in the DmSNAPc-Bdp1-DNA complex. Figure 7 shows the C-terminal domain of DmSNAP190 (residues 543 to 721) modeled in gray color as a nuclear hormone receptor ligand binding domain. This domain of DmSNAP190 was placed in proximity to the Bdp1 SANT domain in an orientation and at a distance that would allow the respective lysines to be cross-linked by BS3.

Finally, DmSNAP43 (blue in Fig. 7) was modeled into the structure. Figure 6B shows that two pivotal BS3 cross-links between DmSNAP43 and TBP were identified. DmSNAP43 residues Lys:284 and Lys:132 cross-linked to TBP residues Lys:257 and Lys:341, respectively. These two TBP lysines lie on the upper surface of TBP in the first and second conserved repeats at positions equivalent to those of yeast TBP residues Lys:145 and Ala:229. To meet those constraints, as well as the constraints of the protein-DNA photo-cross-linking of DmSNAP43 to the PSEA, DmSNAP43 was modeled as an elongated molecule in which more than one region of the protein extended from the PSEA to the upper surface of TBP. The best template identified by RaptorX for the first 265 residues of DmSNAP43 was a family of synthetic helix-loop-helix-loop proteins (41) (*P* value of 3.3e−05); *a priori* modeling was used to generate a structure for the last 98 residues (266 to 363). In each case, the structures were refolded using the flexible loops between the alpha helices. The resulting DmSNAP43 structure is shown in blue in Fig. 7. This structure preserves the protein-DNA cross-linking proximity to the PSEA as well as the proximities of DmSNAP43 Lys:284 and Lys:132 to the respective upper surface residues of TBP.

DISCUSSION

Here, we have proposed a model for the DmSNAPc-Bdp1-TBP complex on the U6 promoter (Fig. 7) that is consistent with EMSA, site-specific protein-DNA photo-cross-linking, and CXMS experiments. Furthermore, the DmSNAPc model shown in Fig. 7 is fully consistent with coimmunoprecipitation experiments that mapped regions of the three DmSNAPc subunits that are required for their assembly with each other (42). The model further provides a rationale for the recruitment of Bdp1 and TBP by DmSNAPc. Bdp1 cross-links to DNA nucleotide positions that extend upstream of the TATA box into positions that are actually a part of the PSEA. These positions are also occupied by DmSNAP190 and DmSNAP43 (but not DmSNAP50), indicating that Bdp1 must lie in close proximity to DmSNAP190 and DmSNAP43. Also supporting this model, our CXMS experiments revealed cross-linking of Bdp1 with DmSNAP190 and DmSNAP43 (but not with DmSNAP50).

Furthermore, we generated additional evidence, beyond that previously published (32), that residues 424 to 510 of Bdp1 are involved in the recruitment of Bdp1 by DmSNAPc. For example, an internal deletion of residues 424 to 510 resulted in the complete loss of Bdp1 recruitment by DmSNAPc (Fig. 2, lane 34 versus lane 35). Moreover, Bdp1 residues 424 to 510 alone exhibited the same pattern as full-length

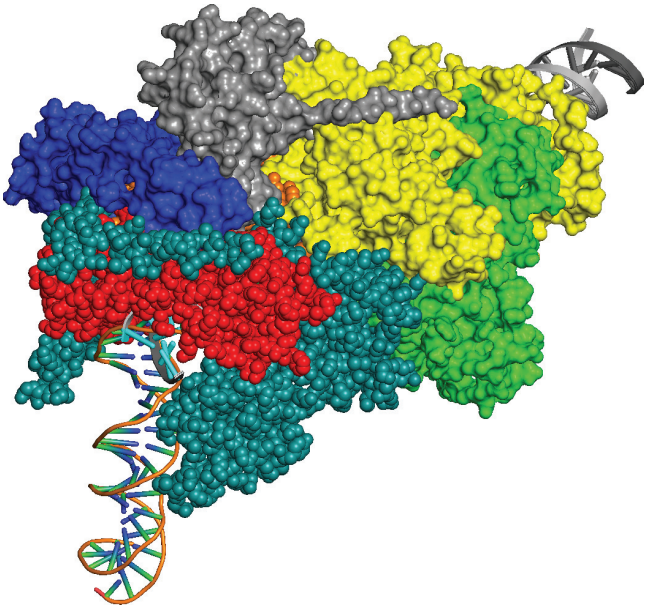

FIG 8 DmSNAPc-Bdp1-TBP-Brf1 structure. This is the same DmSNAPc-Bdp1-TBP structure as that shown in Fig. 7, but it is viewed from a different perspective to better show the location that Brf1 (shown in deep teal) would occupy in the complex. See the text for further discussion.

Bdp1 in site-specific protein-DNA photo-cross-linking (Fig. 5), suggesting that this region of Bdp1 extended into the U6 PSEA, where it would reside in close proximity to DmSNAP190 and DmSNAP43. Finally, the CXMS data with full-length Bdp1 showed that Bdp1 residues 424 to 510, together with nearby residues flanking that region, were responsible for the majority of the protein-protein cross-links between DmSNAPc and Bdp1 (Fig. 6).

In work by others, the N-terminal region of human Bdp1, more so than the C-terminal region, was found to interact with DmSNAPc (35). Interestingly, our CXMS studies revealed that lysines within the N-terminal region of Bdp1 (lysines 203, 206, and 231) cross-link to both DmSNAP190 and DmSNAP43. Thus, it is possible that a region of fly Bdp1 N-terminal of the SANT domain, as well as residues 424 to 510 C-terminal of the SANT domain, interact with DmSNAPc. Perhaps this potential N-terminal interaction of fly Bdp1 with DmSNAPc is not stable enough to be detected in our EMSAs (32).

Interestingly, by EMSA, we have been unable to convincingly demonstrate the existence of a complex that contains both DmSNAPc and Brf1 together with Bdp1 and TBP. Essentially, we see either DmSNAPc-Bdp1-TBP or Brf1-Bdp1-TBP, which lacks DmSNAPc (data not shown). Our modeling suggests a rationale for this result. The finding that a region of DmSNAP43 lies on or near the upper surface of TBP suggests that the binding of DmSNAPc and that of Brf1 are mutually exclusive. Figure 8 shows yeast Brf1 modeled into our proposed SNAPc-Bdp1-TBP complex in accordance with a published cryo-EM structure (17). Depending upon the exact positioning of DmSNAP43, it may sterically or otherwise interfere with the binding of Brf1 along the upper surface of TBP. If this is true, it would suggest some form of regulation to govern the transition from a DmSNAPc-Bdp1-TBP complex to a Brf1-Bdp1-TBP complex.

In light of this potential regulation, we cannot ignore the finding that the C-terminal region of fly DmSNAP190 appears to be structurally related to the ligand-binding domains of members of the nuclear hormone receptor superfamily. The location of this domain (shown in gray color in Fig. 7 and 8), near DmSNAP43 and the SANT domain of Bdp1, raises the intriguing possibility that the activity of *D. melanogaster* SNAPc and the expression of snRNA genes are regulated by an unknown small organic molecule of intracellular or extracellular origin. This could provide an interesting avenue of future research.

The work reported here furthermore suggests pathways toward U6 preinitiation complex assembly in flies and humans that are analogous but different with respect to the intermediary factor that acts as a stabilizing bridge between SNAPc and TBP. In flies, PSEA-bound DmSNAPc recruits Bdp1 in a TATA box-independent manner and TBP in a TATA-dependent manner, with Bdp1 acting to stabilize DmSNAPc and TBP on the PSEA and TATA box, respectively (Fig. 1 and 3). In humans, factor assembly appears to occur analogously but involving Brf2 instead of Bdp1: PSE-bound SNAPc interacts with Brf2 independent of a TATA box, and this complex recruits TBP only in the presence of a TATA box (16, 23). One obvious explanation for the difference is that flies do not have Brf2, so different mechanisms have evolved in flies and humans for TBP recruitment to U6 gene promoters.

In a broader sense, work on snRNA genes by ourselves and others has extended our perspective on the diversity of the TFIIIB components that can be assembled into the Pol III PIC: TBP (for snRNA genes) versus TRF1 (for tRNA and 5S RNA genes) in flies and Brf2 (for snRNA genes) versus Brf1 (for tRNA and 5S RNA genes) in humans. The only constant TFIIIB component known so far is Bdp1. The snRNA work has also revealed different pathways for TFIIIB assembly, at least *in vitro*, on SNAPc-dependent genes versus TFIIIC-dependent genes. The former seem to proceed initially by SNAPc-dependent recruitment of Bdp1 or Brf2, followed by TBP recruitment (this work and reference 23), whereas the latter are thought to occur by TFIIIC-dependent recruitment of TFIIIB either as a preformed complex or proceeding first through Brf1 and TBP recruitment, followed by Bdp1 in a subsequent step (2, 3, 34).

MATERIALS AND METHODS

DmSNAPc, Bdp1, and TBP expression in S2 cells. The preparation of untagged constructs encoding wild-type DmSNAP43, DmSNAP50, and N-terminal His_6-FLAG-tagged DmSNAP190 constructs under the control of the copper-inducible metallothionein promoter has been previously described (42). Expression plasmids for each of the DmSNAPc subunits were used to cotransfect *D. melanogaster* S2 cells as previously described (42). Subunit coexpression was induced with copper sulfate and confirmed by immunoblotting with anti-FLAG M2 monoclonal antibodies (number A9469; Sigma) or antibodies made against synthetic peptides corresponding to amino acid sequence at or near the C terminus of the wild-type proteins (14).

Constructs that encode full-length C-terminal FLAG-Myc-His_6-tagged Bdp1 and C-terminal V5-His_6-tagged TBP under the control of the copper-inducible metallothionein promoter have been previously described (28). FLAG-tagged TBP was prepared by replacing the Myc-His_6 tags in the previous TBP construct with a FLAG tag. The Bdp1 truncation constructs were described previously (32). Expression plasmids were used to generate stably transfected S2 cell lines (42), and copper sulfate-induced expression was confirmed by immunoblotting with anti-V5 monoclonal antibodies (number R960-25; Life Technologies) for TBP detection and anti-FLAG M2 monoclonal antibodies (number A9469; Sigma) for Bdp1 detection.

Nickel-chelate chromatography. Following copper sulfate induction, cells (eight 15-cm-diameter plates per cell line grown to ~100% confluence) were lysed in CelLytic M lysis buffer (number C2978; Sigma) containing 1% protease inhibitor cocktail (number P8340; Sigma). Lysates then were adjusted to a NaCl concentration of 0.5 M prior to incubating with ProBond resin (number R80101; Life Technologies) for 2 h for DmSNAPc and TBP proteins and 30 min for Bdp1 proteins to allow the capture of the His_6-tagged proteins. The resins then were washed three times in 50 mM sodium phosphate buffer (pH 8.0), 0.5 M NaCl, 20 mM imidazole and then once in HEMG-100 buffer (25 mM HEPES K^+ [pH 7.6], 0.1 mM EDTA, 12.5 mM $MgCl_2$, 10 μM $ZnCl_2$, 10% glycerol, 100 mM KCl) containing 0.5 mM phenylmethylsulfonyl fluoride and 20 mM imidazole. The proteins/complexes were eluted from the resin with 750 mM imidazole in HEMG-100 buffer, followed by the addition of 3 mM dithiothreitol to each fraction, and then dialyzed against HEMG-100 buffer containing 1 to 3 mM dithiothreitol.

FLAG immunoaffinity chromatography. Following copper sulfate induction, cells (eight 15-cm-diameter plates per cell line grown to ~100% confluence) were lysed in CelLytic M lysis buffer (number C2978; Sigma) containing 1% protease inhibitor cocktail (number P8340; Sigma). Lysates then were incubated with anti-FLAG M2 affinity gel resin (number A2220; Sigma) at 4°C overnight. On the following day, resins were washed four times in 50 mM Tris and 150 mM NaCl, followed by two washes with HEMG-100 buffer. Proteins were eluted from the resin by incubating in HEMG-100 buffer containing 0.2 mg/ml 3× FLAG peptide (number F4799; Sigma). Elution samples then were dialyzed against HEMG-100 buffer.

EMSAs. EMSAs were performed as previously described (43). Briefly, reactions were carried out in 21-μl volumes in HEMG-100 buffer containing 5 mM dithiothreitol. Each reaction mixture also contained 2 μg of poly(dG-dC) (number P9389; Sigma). Reaction mixtures were incubated with ^{32}P-labeled DNA probe for 30 min at 25°C. The U6 wild-type EMSA probe contained U6:96Ab gene sequence from positions −75 to −7 relative to the transcription start site (sequence shown in Fig. S1 of reference 32).

The mutant probe used in Fig. 3A was identical, except that it contained the sequence GGGACCTC in place of the wild-type TATA sequence TTTATATA. For the oligonucleotide competition experiments shown in Fig. 3B, unlabeled wild-type and mutant oligonucleotides were used that were similar to those described above, except that they contained U6 DNA sequence only between nucleotide positions −42 and −7 in order to exclude the PSEA. For antibody-induced supershifts, the antibodies were added halfway through the 30-min incubation. Complexes then were run on 4% nondenaturing polyacrylamide gels in 25 mM Tris, 190 mM glycine, 1 mM EDTA (pH 8.3) and detected by autoradiography. Relative band intensities were quantitated by using Image Studio software from LI-COR Biosciences.

Site-specific protein-DNA photo-cross-linking. DNA probes for site-specific protein-DNA photo-cross-linking reactions were prepared as previously described in detail (29). Twenty-eight individual double-stranded DNA probes (14 on the template strand and 14 on the nontemplate strand; Fig. 4) were prepared that incorporated a photo-cross-linking agent (azidophenacyl group) at specific individual phosphate positions 22 to 49 nucleotides upstream of the transcription start site of the U6 snRNA gene. Each probe also contained a ^{32}P radiolabel at the second nucleotide 5′ of the cross-linker. Photo-cross-linking reactions were performed as previously described in detail (33). Briefly, 100,000 cpm of DNA probe was incubated with FLAG- or Ni-purified proteins in the dark for 30 min, followed by 313-nm UV irradiation. Samples were digested with DNase I and S1 nuclease, and cross-linked proteins were identified by denaturing polyacrylamide gel electrophoresis followed by autoradiography.

CXMS of transcription factor complexes on U6 promoter DNA. For the CXMS analyses of the DmSNAPc-Bdp1-U6 promoter complex and the DmSNAPc-Bdp1-TBP-U6 promoter complex, approximately 25 pmol of FLAG-purified DmSNAPc, 325 pmol of untagged Bdp1 (expressed in *Escherichia coli* by GenScript), and 312 pmol of U6 promoter DNA (sequence from −75 to −7) were mixed together, with or without 450 pmol of FLAG-purified TBP, in a final volume of 1 ml in HEMG buffer containing 2 mM dithiothreitol. Following a 25°C incubation for 30 min, bis(sulfosuccinimidyl)suberate (BS3) (number 21585; Thermo Fisher) was added to a final concentration of 2 mM and incubated for 1 h at 25°C, followed by the addition of ammonium bicarbonate to 20 mM for an additional 5 min. Sample preparation for CXMS and identification of cross-linked peptides were carried out as previously described (44). Cross-linking spectra and maps can be viewed at https://www.yeastrc.org/proxl_public/viewProject.do?project_id=66.

Structure generation and representation. Structures of DmSNAPc subunits and of *D. melanogaster* Bdp1 were generated by using the RaptorX structure prediction program (37), and images were prepared by using PyMOL (Schrodinger LLC).

ACKNOWLEDGMENTS

This work was supported by the National Science Foundation (MCB-1616487) and by the California Metabolic Research Foundation.

We thank Phil Gafken and Lisa Jones at the Fred Hutchinson Cancer Research Center proteomics facility for mass spectrometry analyses.

REFERENCES

1. Willis IM. 1993. RNA polymerase III. Genes, factors and transcriptional specificity. Eur J Biochem 212:1–11. https://doi.org/10.1111/j.1432-1033.1993.tb17626.x.
2. Geiduschek EP, Kassavetis GA. 2001. The RNA polymerase III transcription apparatus. J Mol Biol 310:1–26. https://doi.org/10.1006/jmbi.2001.4732.
3. Schramm L, Hernandez N. 2002. Recruitment of RNA polymerase III to its target promoters. Genes Dev 16:2593–2620. https://doi.org/10.1101/gad.1018902.
4. Kunkel GR, Maser RL, Calvet JP, Pederson T. 1986. U6 small nuclear RNA is transcribed by RNA polymerase III. Proc Natl Acad Sci U S A 83:8575–8579. https://doi.org/10.1073/pnas.83.22.8575.
5. Murphy S, Di Liegro C, Melli M. 1987. The in vitro transcription of the 7SK RNA gene by RNA polymerase III is dependent only on the presence of an upstream promoter. Cell 51:81–87. https://doi.org/10.1016/0092-8674(87)90012-2.
6. Baer M, Nilsen TW, Costigan C, Altman S. 1990. Structure and transcription of a human gene for H1 RNA, the RNA component of human RNase P. Nucleic Acids Res 18:97–103. https://doi.org/10.1093/nar/18.1.97.
7. Carbon P, Krol A. 1991. Transcription of the Xenopus laevis selenocysteine tRNA(Ser)Sec gene: a system that combines an internal B box and upstream elements also found in U6 snRNA genes. EMBO J 10:599–606. https://doi.org/10.1002/j.1460-2075.1991.tb07987.x.
8. Yuan Y, Reddy R. 1991. 5′ Flanking sequences of human MRP/7–2 RNA gene are required and sufficient for the transcription by RNA polymerase III. Biochim Biophys Acta 1089:33–39. https://doi.org/10.1016/0167-4781(91)90081-V.
9. Myslinski E, Ame JC, Krol A, Carbon P. 2001. An unusually compact external promoter for RNA polymerase III transcription of the human H1RNA gene. Nucleic Acids Res 29:2502–2509. https://doi.org/10.1093/nar/29.12.2502.
10. Jawdekar GW, Henry RW. 2008. Transcriptional regulation of human small nuclear RNA genes. Biochim Biophys Acta 1779:295–305. https://doi.org/10.1016/j.bbagrm.2008.04.001.
11. Hung KH, Stumph WE. 2011. Regulation of snRNA gene expression by the Drosophila melanogaster small nuclear RNA activating protein complex (DmSNAPc). Crit Rev Biochem Mol Biol 46:11–26. https://doi.org/10.3109/10409238.2010.518136.
12. Murphy S, Yoon JB, Gerster T, Roeder RG. 1992. Oct-1 and Oct-2 potentiate functional interactions of a transcription factor with the proximal sequence element of small nuclear RNA genes. Mol Cell Biol 12:3247–3261. https://doi.org/10.1128/MCB.12.7.3247.
13. Sadowski CL, Henry RW, Lobo SM, Hernandez N. 1993. Targeting TBP to a non-TATA box cis-regulatory element: a TBP-containing complex activates transcription from snRNA promoters through the PSE. Genes Dev 7:1535–1548. https://doi.org/10.1101/gad.7.8.1535.
14. Li C, Harding GA, Parise J, McNamara-Schroeder KJ, Stumph WE. 2004. Architectural arrangement of cloned proximal sequence element-binding protein subunits on Drosophila U1 and U6 snRNA gene promoters. Mol Cell Biol 24:1897–1906. https://doi.org/10.1128/MCB.24.5.1897-1906.2004.
15. Egloff S, O'Reilly D, Murphy S. 2008. Expression of human snRNA genes from beginning to end. Biochem Soc Trans 36:590–594. https://doi.org/10.1042/BST0360590.
16. Dergai O, Cousin P, Gouge J, Satia K, Praz V, Kuhlman T, Lhote P, Vannini A, Hernandez N. 2018. Mechanism of selective recruitment of RNA

polymerases II and III to snRNA gene promoters. Genes Dev 32:711–722. https://doi.org/10.1101/gad.314245.118.
17. Vorlander MK, Khatter H, Wetzel R, Hagen WJH, Muller CW. 2018. Molecular mechanism of promoter opening by RNA polymerase III. Nature 553:295–300. https://doi.org/10.1038/nature25440.
18. Takada S, Lis JT, Zhou S, Tjian R. 2000. A TRF1:BRF complex directs Drosophila RNA polymerase III transcription. Cell 101:459–469. https://doi.org/10.1016/S0092-8674(00)80857-0.
19. Verma N, Hung KH, Kang JJ, Barakat NH, Stumph WE. 2013. Differential utilization of TATA box-binding protein (TBP) and TBP-related factor 1 (TRF1) at different classes of RNA polymerase III promoters. J Biol Chem 288:27564–27570. https://doi.org/10.1074/jbc.C113.503094.
20. Gouge J, Satia K, Guthertz N, Widya M, Thompson AJ, Cousin P, Dergai O, Hernandez N, Vannini A. 2015. Redox signaling by the RNA polymerase III TFIIB-related factor Brf2. Cell 163:1375–1387. https://doi.org/10.1016/j.cell.2015.11.005.
21. Henry RW, Sadowski CL, Kobayashi R, Hernandez N. 1995. A TBP-TAF complex required for transcription of human snRNA genes by RNA polymerases II and III. Nature 374:653–656. https://doi.org/10.1038/374653a0.
22. Yoon JB, Murphy S, Bai L, Wang Z, Roeder RG. 1995. Proximal sequence element-binding transcription factor (PTF) is a multisubunit complex required for transcription of both RNA polymerase II- and RNA polymerase III-dependent small nuclear RNA genes. Mol Cell Biol 15:2019–2027. https://doi.org/10.1128/MCB.15.4.2019.
23. Dergai O, Hernandez N. 2019. How to recruit the correct RNA polymerase? Lessons from snRNA genes. Trends Genet 35:457–469. https://doi.org/10.1016/j.tig.2019.04.001.
24. Lai HT, Kang YS, Stumph WE. 2008. Subunit stoichiometry of the Drosophila melanogaster small nuclear RNA activating protein complex (SNAPc). FEBS Lett 582:3734–3738. https://doi.org/10.1016/j.febslet.2008.09.059.
25. Ma BC, Hernandez N. 2002. Redundant cooperative interactions for assembly of a human U6 transcription initiation complex. Mol Cell Biol 22:8067–8078. https://doi.org/10.1128/MCB.22.22.8067-8078.2002.
26. Hinkley CS, Hirsch HA, Gu LP, LaMere B, Henry RW. 2003. The small nuclear RNA-activating protein 190 Myb DNA binding domain stimulates TATA box-binding protein-TATA box recognition. J Biol Chem 278:18649–18657. https://doi.org/10.1074/jbc.M204247200.
27. Reference deleted.
28. Kang JJ, Kang YS, Stumph WE. 2016. TFIIIB subunit locations on U6 gene promoter DNA mapped by site-specific protein-DNA photo-cross-linking. FEBS Lett 590:1488–1497. https://doi.org/10.1002/1873-3468.12185.
29. Kim MK, Kang YS, Lai HT, Barakat NH, Magante D, Stumph WE. 2010. Identification of SNAPc subunit domains that interact with specific nucleotide positions in the U1 and U6 gene promoters. Mol Cell Biol 30:2411–2423. https://doi.org/10.1128/MCB.01508-09.
30. Doherty MT, Kang YS, Lee C, Stumph WE. 2012. Architectural arrangement of the small nuclear RNA (snRNA)-activating protein complex 190 subunit (SNAP190) on U1 snRNA gene promoter DNA. J Biol Chem 287:39369–39379. https://doi.org/10.1074/jbc.M112.407775.
31. Kang YS, Kurano M, Stumph WE. 2014. The Myb domain of the largest subunit of SNAPc adopts different architectural configurations on U1 and U6 snRNA gene promoter sequences. Nucleic Acids Res 42:12440–12454. https://doi.org/10.1093/nar/gku905.
32. Verma N, Hurlburt AM, Wolfe A, Kim MK, Kang YS, Kang JJ, Stumph WE. 2018. Bdp1 interacts with SNAPc bound to a U6, but not U1, snRNA gene promoter element to establish a stable protein-DNA complex. FEBS Lett 592:2489–2498. https://doi.org/10.1002/1873-3468.13169.
33. Wang Y, Stumph WE. 1998. Identification and topological arrangement of Drosophila proximal sequence element (PSE)-binding protein subunits that contact the PSEs of U1 and U6 snRNA genes. Mol Cell Biol 18:1570–1579. https://doi.org/10.1128/MCB.18.3.1570.
34. Male G, von Appen A, Glatt S, Taylor NMI, Cristovao M, Groetsch H, Beck M, Müller CW. 2015. Architecture of TFIIIC and its role in RNA polymerase III pre-initiation complex assembly. Nat Commun 6:7387. https://doi.org/10.1038/ncomms8387.
35. Gouge J, Guthertz N, Kramm K, Dergai O, Abascal-Palacios G, Satia K, Cousin P, Hernandez N, Grohmann D, Vannini A. 2017. Molecular mechanisms of Bdp1 in TFIIIB assembly and RNA polymerase III transcription initiation. Nat Commun 8:130. https://doi.org/10.1038/s41467-017-00126-1.
36. Abascal-Palacios G, Ramsay EP, Beuron F, Morris E, Vannini A. 2018. Structural basis of RNA polymerase III transcription initiation. Nature 553:301–306. https://doi.org/10.1038/nature25441.
37. Kallberg M, Wang H, Wang S, Peng J, Wang Z, Lu H, Xu J. 2012. Template-based protein structure modeling using the RaptorX web server. Nat Protoc 7:1511–1522. https://doi.org/10.1038/nprot.2012.085.
38. Jaiswal R, Choudhury M, Zaman S, Singh S, Santosh V, Bastia D, Escalante CR. 2016. Functional architecture of the Reb1-Ter complex of Schizosaccharomyces pombe. Proc Natl Acad Sci U S A 113:E2267–E2676. https://doi.org/10.1073/pnas.1525465113.
39. Hardin SB, Ortler CJ, McNamara-Schroeder KJ, Stumph WE. 2000. Similarities and differences in the conformation of protein-DNA complexes at the U1 and U6 snRNA gene promoters. Nucleic Acids Res 28:2771–2778. https://doi.org/10.1093/nar/28.14.2771.
40. Hernandez G, Valafar F, Stumph WE. 2007. Insect small nuclear RNA gene promoters evolve rapidly yet retain conserved features involved in determining promoter activity and RNA polymerase specificity. Nucleic Acids Res 35:21–34. https://doi.org/10.1093/nar/gkl982.
41. Brunette TJ, Parmeggiani F, Huang PS, Bhabha G, Ekiert DC, Tsutakawa SE, Hura GL, Tainer JA, Baker D. 2015. Exploring the repeat protein universe through computational protein design. Nature 528:580–584. https://doi.org/10.1038/nature16162.
42. Hung KH, Titus M, Chiang SC, Stumph WE. 2009. A map of Drosophila melanogaster small nuclear RNA-activating protein complex (DmSNAPc) domains involved in subunit assembly and DNA binding. J Biol Chem 284:22568–22579. https://doi.org/10.1074/jbc.M109.027961.
43. Hung KH, Stumph WE. 2012. Localization of residues in a novel DNA-binding domain of DmSNAP43 required for DmSNAPc DNA-binding activity. FEBS Lett 586:841–846. https://doi.org/10.1016/j.febslet.2012.02.009.
44. Mashtalir N, D'Avino AR, Michel BC, Luo J, Pan J, Otto JE, Zullow HJ, McKenzie ZM, Kubiak RL, St Pierre R, Valencia AM, Poynter SJ, Cassel SH, Ranish JA, Kadoch C. 2018. Modular organization and assembly of SWI/SNF family chromatin remodeling complexes. Cell 175:1272–1288. https://doi.org/10.1016/j.cell.2018.09.032.
45. Jensen RC, Wang Y, Hardin SB, Stumph WE. 1998. The proximal sequence element (PSE) plays a major role in establishing the RNA polymerase specificity of Drosophila U-snRNA genes. Nucleic Acids Res 26:616–622. https://doi.org/10.1093/nar/26.2.616.
46. McNamara-Schroeder KJ, Hennessey RF, Harding GA, Jensen RC, Stumph WE. 2001. The Drosophila U1 and U6 gene proximal sequence elements act as important determinants of the RNA polymerase specificity of snRNA gene promoters in vitro and in vivo. J Biol Chem 276:31786–31792. https://doi.org/10.1074/jbc.M101273200.
47. Barakat NH, Stumph WE. 2008. TBP recruitment to the U1 snRNA gene promoter is disrupted by substituting a U6 proximal sequence element A (PSEA) for the U1 PSEA. FEBS Lett 582:2413–2416. https://doi.org/10.1016/j.febslet.2008.06.003.